Simulation and Computation of Hypersonic Flow Characteristics over a wedge using Ideal Gas and Bose-Einstein Models

Eric Qiu

Guggenheim School of Aerospace Engineering, Georgia Institute of Technology

AE 6015: Advanced Aerodynamics

Dr. Lakshmi N. Sankar

April 10, 2022

Introduction

The subject of interest of this report is the hypersonic flow behavior around a standard wedge-like object (Figure 1), referring to the shock angle created by the flow relative to the cone wedge angle. The approach consists of two separate but related parts – an ideal gas flow computation and a real gas flow computation (see Procedure). The ideal gas flow computation iteratively solves for shock angle using a given wedge angle, like Assignment 4. The real gas flow computation uses the previous ideal approximation as initial values, iteratively solving for new thermodynamic properties according to real gas behavior until convergence. The results are then compared against empirical data for verification and presented in Results section. A brief Conclusion is also drawn about hypersonic flows.

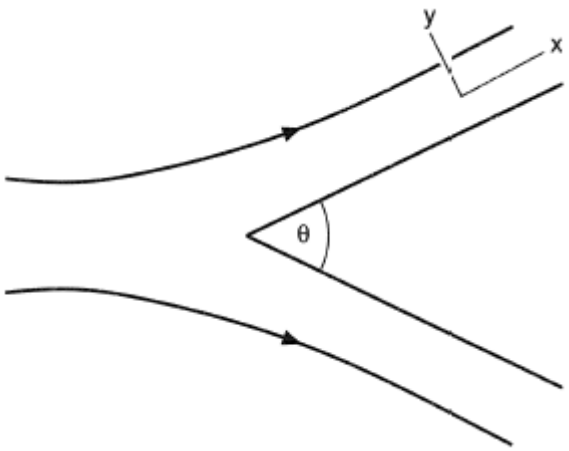

Figure 1: Hypersonic flow characteristics around wedge of angle theta

Procedure

As stated, the procedure is divided into two parts- an ideal and a real gas simulation. Beginning with the ideal portion (as it is the basis for the real gas portion), we are given M_1, δ_s - the Mach number of the freestream and the wedge deflection angle respectively. Using these given values, we solve for β, the shock angle produced by the flow, which may then be used to solve for M_2, the Mach number behind the shock wave. Further, this also gives us enough information to solve for pressure and temperature ratios across the shock wave. These are represented in Eq.1-Eq.5 respectively.

$$Eq.1: \delta_s = \arctan\left(\cot\beta * \frac{M_1^2 \sin^2\beta - 1}{\frac{\gamma+1}{2} M_1^2 - (M_1^2 \sin^2\beta - 1)}\right)$$

$$Eq.2: M_2^2 = \frac{1 + \frac{\gamma - 1}{2} M_1^2}{\gamma M_1^2 \sin^2 \beta - \frac{\gamma - 1}{2}} + \frac{M_1^2 \cos^2 \beta}{1 + \frac{\gamma - 1}{2} M_1^2 \sin^2 \beta}$$

$$Eq.3: \frac{\rho_2}{\rho_1} = \frac{(\gamma + 1)(M_1 sin\beta)^2}{(\gamma - 1)(M_1 sin\beta)^2 + 2}$$

$$Eq.4: \frac{P_2}{P_1} = 1 + \frac{2\gamma}{\gamma + 1}((M_1 sin\beta)^2 - 1)$$

$$Eq.5: \frac{T_2}{T_1} = \frac{P_2}{P_1} * \frac{\rho_1}{\rho_2}$$

Now, the problem with the ideal gas approximation is that the thermodynamic properties of the gas are changing across the shock, which is not being accounted for. To rectify this, in the real gas portion (Bose-Einstein model) of this procedure, we define $f(T_2, u_2), g(T_2, u_2)$, two modeling equations for the gas behind the shock. These are given in Eq.6 and Eq.7. In these equations, the subscript "1" denotes the thermodynamic state of the gas before the shock wave, and the subscript "2" denotes the same for behind the shock wave. Note that T_r is the Einstein temperature, 3070 K.

$$Eq.6: f(T_2, u_2) = T_2 + \frac{u_2^2}{2c_p} + \frac{\gamma - 1}{\gamma}\left(\frac{T_r}{e^{\frac{T_r}{T2}} - 1}\right) - (T_1 + \frac{(u_1 sin\beta)^2}{2c_p} + \frac{\gamma - 1}{\gamma}(\frac{T_r}{e^{\frac{T_r}{T_2}} - 1})$$

$$Eq.7: g(T_2, u_2) = T_2 + \frac{u^2}{R_g} - \left[T_1 + \frac{(u_1 sin\beta)^2}{R_g}\right]\left(\frac{u_2}{u_1 sin\beta}\right)$$

The procedure involves computing the Jacobian matrix of Eq.6 and Eq.7, presented below.

$$Eq.8: J = \begin{bmatrix} \frac{\partial f}{\partial T_2} & \frac{\partial f}{\partial u_2} \\ \frac{\partial g}{\partial T_2} & \frac{\partial g}{\partial u_2} \end{bmatrix}$$

Then, iteratively, we solve for the convergence of temperature and speed T_2, u_2 until the exit condition Eq.10 is satisfied. Note that different values of ϵ can be utilized to varying effect. For this assignment's purposes, a value of 0.01 was deemed sufficiently small.

$$Eq.9: T_2^{n+1} = T_2^n - \frac{f(T_2,u_2) * \frac{\partial g}{\partial u_2} - g(T_2,u_2) * \frac{\partial f}{\partial u_2}}{\frac{\partial f}{\partial T_2} * \frac{\partial g}{\partial u_2} - \frac{\partial f}{\partial u_2} * \frac{\partial g}{\partial T_2}}$$

$$Eq.10: u_2^{n+1} = u_2^n - \frac{g(T_2,u_2) * \frac{\partial f}{\partial T_2} - f(T_2,u_2) * \frac{\partial g}{\partial T_2}}{\frac{\partial f}{\partial T_2} * \frac{\partial g}{\partial u_2} - \frac{\partial f}{\partial u_2} * \frac{\partial g}{\partial T_2}}$$

$$Eq.11: \sqrt{\left(\frac{u_2^{n+1} - u_2^n}{u_2^n}\right)^2 + \left(\frac{T_2^{n+1} - T_2^n}{T_2^n}\right)^2} < \epsilon$$

From this iterative loop we obtain converged values of T_2, u_2. From there, it is simple to obtain the necessary outputs (Eq.12 -15).

$$Eq.12: \beta_n = \beta - \frac{1}{1 - 0.5\sin\big(2(\beta-\theta)\big)\tan\beta} * (\arctan\left(\frac{u_1 sin\beta - u_2}{u_1\cos\beta + u_2 tan\beta}\right) - \theta)$$

$$Eq.13: \gamma_2 = \frac{\left[\frac{7}{2} + \frac{e^{\frac{T_r}{T}}\left(\frac{T_r}{T}\right)^2}{\left(e^{\frac{T_r}{T}} - 1\right)^2}\right] R_g}{\left[\frac{5}{2} + \frac{e^{\frac{T_r}{T}}\left(\frac{T_r}{T}\right)^2}{\left(e^{\frac{T_r}{T}} - 1\right)^2}\right] R_g}$$

$$Eq.14: M_2 = \frac{\frac{u_2}{\sin(\beta_n - \theta)}}{\sqrt{\gamma_2 * R_g * T_2}}$$

$$Eq.15: \frac{p_2}{p_1} = \frac{1 + \gamma_1 (M_1 sin\beta)^2}{1 + \gamma_2 (M_2 \sin(\beta - \theta))^2}$$

Implementation of these equations in the MATLAB code directly led to the results following in the next section of this report.

Results

The analysis is performed for the following values: $M_1 = 4, 8, 12, 16, 24$ and $\theta_c = 15°$. The results are presented in tabular form below (Table 1 and 3). The accepted AIAA results are presented in Tables 2 and 4 for comparison.

M_1	β(degrees)	M_2	$\frac{T_2}{T_1}$	$\frac{T_{02}}{T_{01}}$	$\frac{p_2}{p_1}$
4	27.0629	2.9290	1.5465	1	3.6973
8	20.8605	4.7477	2.5053	1	9.3013
12	19.4146	5.6548	4.0294	1	18.3957
16	18.8670	6.1218	6.1445	1	31.0647
24	18.4594	6.5374	12.1707	1	67.2055

Table 1: Experimental hypersonic flow characteristics under ideal gas assumptions

M_1	β(degrees)	M_2	$\frac{T_2}{T_1}$	$\frac{T_{02}}{T_{01}}$	$\frac{p_2}{p_1}$
4	27.0711	2.9271	1.5483	1	3.7004
8	20.8691	4.7425	2.5107	1	9.3117
12	19.4234	5.6469	4.0406	1	18.4181
16	18.8760	6.1121	6.1637	1	31.1043
24	18.4687	6.5258	12.2129	1	67.2941

Table 2: Accepted hypersonic flow characteristics under ideal gas assumptions

M_1	β(degrees)	M_2	$\frac{T_2}{T_1}$	$\frac{T_{02}}{T_{01}}$	$\frac{p_2}{p_1}$
4	27.0452	2.9314	1.5397	0.9954	3.6976
8	20.7612	4.8210	2.4684	0.9692	9.2669
12	19.2218	5.9185	3.8365	0.9024	18.2332
16	18.5264	6.6049	5.6049	0.8574	30.5435
24	17.8893	7.4293	10.1966	0.8092	65.2451

Table 3: Experimental hypersonic flow characteristics under real gas model

M_1	β(degrees)	M_2	$\frac{T_2}{T_1}$	$\frac{T_{02}}{T_{01}}$	$\frac{p_2}{p_1}$
4	27.0560	2.9307	1.5454	0.9968	3.6988
8	20.7759	4.8136	2.4702	0.9695	9.2743
12	19.2225	5.8959	3.8579	0.9091	18.2390
16	18.5269	6.6041	5.6132	0.8581	30.5535
24	17.8974	7.4285	10.2179	0.8095	65.2719

Table 4: Accepted hypersonic flow characteristics under real gas model

Conclusion

The main takeaways from the data are:

1) The flow is faster in the real gas model than the ideal gas approximation.
2) The temperature and pressure are both lower in the real gas model than the ideal gas approximation.
3) The shock angles are smaller in the real gas model than the ideal gas approximation.
4) These effects are exacerbated as Mach number increases.

A simple explanation can be found in the 4th column of all four tables – that is, the stagnation temperature ratio. In the ideal gas assumption, we keep c_p, c_v independent of temperature. Hence, the process is isentropic and behaves as such. In the real gas simulation, the total energy of the gas is not constant as we consider varying c_p, c_v – therefore, the process is not isentropic and some of the energy is converted to heat. It is thus expected that pressure and temperature (as well as density) are lower.

As a side-effect of this relationship, the flow also speeds up, although very slightly, and the shock angle is slightly lower. Due to the ideal gas assumption not ever truly completely holding up, we expect the real gas values to be the more accurate of the two sets presented here.

References

1. Sankar, Lakshmi N. (2021). *Assignment 5 Notes.* Georgia Institute of Technology, Guggenheim School of Aerospace Engineering.
2. Whitmore, S. A. (2007). Real Gas Extensions to Tangent-Wedge and Tangent-Cone Analysis Methods. In AIAA Journal (Vol. 45, Issue 8, pp. 2024–2032). American Institute of Aeronautics and Astronautics (AIAA). https://doi.org/10.2514/1.28521